Available online at www.sciencedirect.com
ScienceDirect
Applied Geochemistry 23 (2008) 914–931
Applied Geochemistry
www.elsevier.com/locate/apgeochem

Geochemical characterization of surface waters and groundwater resources in the Managua area (Nicaragua, Central America)

F. Parello [a,*], A. Aiuppa [a], H. Calderon [b], F. Calvi [c], D. Cellura [a], V. Martinez [b], M. Militello [a], K. Vammen [b], D. Vinti [a]

[a] *Dipartimento di Chimica e Fisica della Terra, Università di Palermo, Via Archirafi 36, 90123 Palermo, Italy*
[b] *Centro para la Investigaciòn en Recursos Acuàticos de Nicaragua UNAN. Apartado Postal 4598, Managua, Nicaragua*
[c] *Via C. De Grossis 2, 90135 Palermo, Italy*

Received 27 November 2006; accepted 22 August 2007
Editorial handling by H. Armannsson
Available online 15 January 2008

Abstract

This paper reports new geochemical data on dissolved major and minor constituents in surface waters and ground waters collected in the Managua region (*Nicaragua*), and provides a preliminary characterization of the hydrogeochemical processes governing the natural water evolution in this area. The peculiar geological features of the study site, an active tectonic region (Nicaragua Depression) characterized by active volcanism and thermalism, combined with significant anthropogenic pressure, contribute to a complex evolution of water chemistry, which results from the simultaneous action of several geochemical processes such as evaporation, rock leaching, mixing with saline brines of natural or anthropogenic origin. The effect of active thermalism on both surface waters (e.g., saline volcanic lakes) and groundwaters, as a result of mixing with variable proportions of hyper-saline geothermal Na–Cl brines (e.g., Momotombo geothermal plant), accounts for the high salinities and high concentrations of many environmentally-relevant trace elements (As, B, Fe and Mn) in the waters. At the same time the active extensional tectonics of the Managua area favour the interaction with acidic, reduced thermal fluids, followed by extensive leaching of the host rock and the groundwater release of toxic metals (e.g., Ni, Cu). The significant pollution in the area, deriving principally from urban and industrial waste-water, probably also contributes to the aquatic cycling of many trace elements, which attain concentrations above the WHO recommended limits for the elements Ni (~40 μg/l) and Cu (~10 μg/l) limiting the potential utilisation of Lake Xolotlan for nearby Managua.

1. Introduction

Nicaragua, a large developing country in Central America (130,682 km^2), is covered to the extent of approximately 10% by surface waters. Two main hydrological basins, lakes Managua (Xolotlan, 1053 km^2) and Nicaragua (Cocibolca, 8144 km^2), are located in the Rio San Juan Basin, the largest in the country (29.824 km^2). These two lakes, collecting an average precipitation of 1694 mm/year, could provide a huge water supply for the

* Corresponding author. Fax: +39 0916168376.
E-mail address: parello@unipa.it (F. Parello).

0883-2927/$ - see front matter © 2008 Elsevier Ltd. All rights reserved.
doi:10.1016/j.apgeochem.2007.08.006

neighbouring cities. Unfortunately, these immense resources are counterbalanced by a general degradation of water quality, mostly due to indiscriminate and un-regulated urban and industrial waste water removal, and un-controlled rural and agricultural activities. Furthermore, the Managua area is peculiar from a geological and structural point of view, lying in the Miocenic Nicaragua depression, and with the trans-extensive, N–S trending Nejapa-Miraflores tectonic lineament running along its western edge (Fig. 1). This lineament intersects and shifts the Central American Quaternary volcanic arc over a length of about 15 km, and is the site of widespread Holocene volcanism (Walker, 1984), active thermalism and seismic activity (Burkart and Self, 1985). Thus, as in other active volcanic/tectonic areas (e.g., Aiuppa et al., 2003a), a profound impact of volcanic activity on surface and ground water chemistry can be expected, due to the anomalous heat and/or mass contribution of magmatic/hydrothermal fluids. This may alter the quality of water in many ways (Delmelle, 2003), by favouring the development of extreme temperature, pH, and redox conditions and, by fostering intense gas–water–rock interaction, resulting in high-salinity waters or directly adding dangerous or toxic chemicals (Aiuppa et al., 2003b). The main objective of this work is the elucidation of the principal hydro-geochemical processes that govern the evolution of the natural waters in the study area, with a special

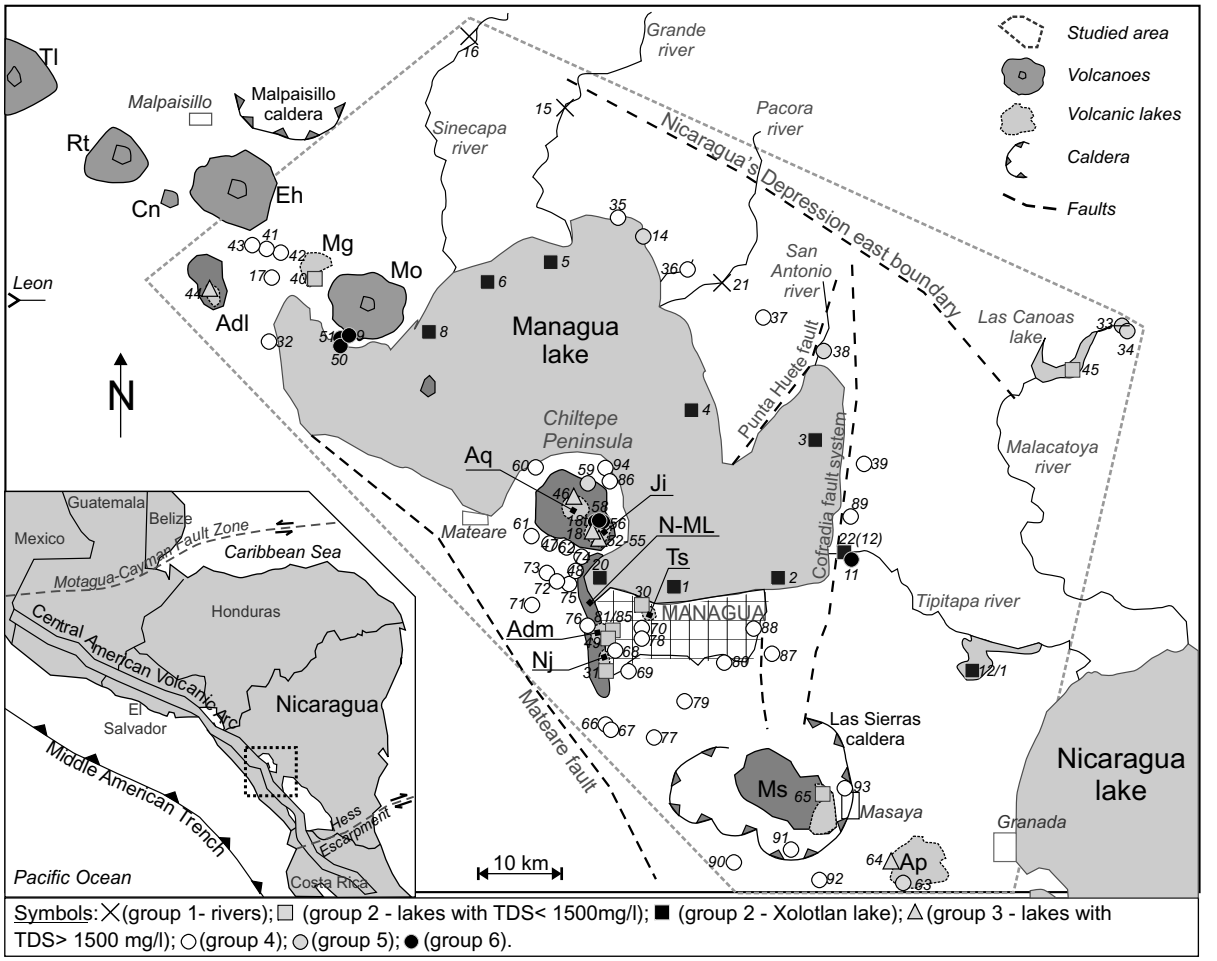

Fig. 1. Sketch map of the sampled area around the Managua lake with location of samples, main tectonic lineaments (after van Wyk de Vries, 1993) and the volcanic centres: Adl (Asososca de Leon), Adm (Asososca de Managua), Ap (Apoyo), Aq (Apoyeque), Cn (CerroNegro), Eh (El Hoyo) Ji (Jiloa), Mg (Monte Galan), Mo (Momotombo), Ms (Masaya), Nj (Nejapa), NML (Nejapa-Miraflores Lineament), Rt (Rota), Tl (Telica), Ts (Tiscapa). In the inset on the left the regional tectonic setting of Nicaragua, with the active Central American volcanic chain.

interest in the characterization of possible interaction between groundwaters and volcanic and/or geothermal fluids.

The main results of a hydro-geochemical survey carried out in the Managua region between June 2002 and July 2003, are reported providing new data on the abundance of major, minor, and trace inorganic constituents in a set of ~100 water samples, including surface waters and groundwaters. An attempt is made to provide an initial characterization of the geochemical processes governing the chemical features of surface water and groundwater in the area, and to outline the relative importance of natural versus anthropogenic factors in the degradation of water quality.

2. The study area, materials and methods

2.1. Geodynamics and volcanic activity

The geodynamics of Central America is characterized by the collision of the Caribbean and Cocos plates, with the latter subducting at an average rate of 8 cm/a (DeMets, 2001). This process is responsible for the widespread Tertiary and Quaternary volcanism in the area and the intense seismic activity. The contact between the two plates is marked by the "Middle American Trench", extending NW-SE from Mexico to Costa Rica. The Teuantepec Ridge divides the trench into two blocks characterized by different rates of movement (Couch and Woodcock, 1981). The main regional tectonic structure of western Nicaragua, the 70–80 km wide Nicaragua Depression, runs parallel to the Middle American Trench for about 300 km. This depression evolved during a change in the slope of the slab in late Miocene (Martinez and Noguera, 1992). In the Managua district, the two main tectonic structures are the Managua graben and the horst Pueblos Height, which are interpreted as an extensional basin and a pressure ridge, respectively (Aydin and Nur, 1982). The Managua graben is the site of considerable seismic and volcano-tectonic activity. It is ~40 km long (N–S direction) and 25 km wide; its western boundary is marked by the Mateare fault, which extends about 52 km towards N20° − 30 °W (Fig. 1). The Nicaragua NW-SE-trending volcanic arc is situated in the NW segment of the Central American volcanic chain, and extends for about 400 km. Volcanic activity started about 100 ka ago in the inland plateau, and shifted westwards during the Quaternary (Carr et al., 2003). The volcanic arc is currently made up of 12 active volcanic structures. It is divided into two parallel segments by the Nejapa-Miraflores secondary line with a N–S direction, with an estimated dislocation of 15–20 km. The NW volcanic chain extends for about 175 km, from the Cosiguina volcano in the Fonseca Gulf on the border with Honduras to the Momotombo volcano and the small Apoyeque caldera; the SW volcanic chain extends for 215 km from Masaya volcano to Madera volcano and Conception volcano, which formed Ometepe Island in Nicaragua lake. Volcanic products range in composition from tholeiitic basalts to calc-alkaline acid and intermediate rocks (McBirney and Williams, 1965; Carr, 1984; Walker et al., 1990; van Wyk de Vries, 1993).

The study area is bordered in the north by the volcanic lake of Asososca de Leon, and in the south by the volcanic lake of Apoyo, the largest of the recent calderas in Nicaragua (Fig. 1). Masaya and Momotombo are the main active volcanoes in the area. The first (6.5 ka old) is an active basaltic shield volcano situated 25 km south-east of Managua. It has exhibited several episodes of passive degassing since 1852 until now; present degassing crisis starting in mid-1993. Momotombo is 4.5 ka old basaltic-andesitic stratovolcano, among the most active in Central America (Istituto Vulcanologico A.C., U.R.S.S, 1983). In the centre of the studied area, 6 km north of the city of Managua, the Chiltepe peninsula extends in an almost rounded shape into the Managua lake, and has the shape of the eroded remains of a low shield volcano. The morphology of the volcano reveals a complex evolution, by initial central effusive activity to a typical explosive volcanism, creating the two main structures: the Apoyeque (central) and Jiloa (secondary) calderas and minor volcanic centres such as cinder cones and lava domes.

2.2. Hydrogeology

The surface area of Lake Xolotlán, situated close to Managua, is 1050 km^2, its length 58 km, its maximum width 32 km and its average depth about 9.5 m. The estimated volume of water is about 10^{10} m^3 and the maximum depth 30 m. The lake occupies a part of the Nicaragua graben, and it lies over the "Sierra of Managua" volcanic formation. Until 1910, the lake flowed out through the river Tipitapa (Fig. 1) into the Nicaragua lake. In the course of time, the discharge was interrupted, due to the subsidence of the water level of the Managua lake. The water level has only recently been

Table 1
Chemical analyses of major elements determined by ion chromatography. Temperature, pH, Eh and conductivity were measured in the field with portable instruments

Samples	*T* (°C)	TDS (mg/l)	Cond (μS)	pH	Eh	Na (mg/l)	K (mg/l)	Mg (mg/l)	Ca (mg/l)	F (mg/l)	Cl (mg/l)	SO_4 (mg/l)	HCO_3 (mg/l)
Group 1 (rivers)													
15	31	172	183	8.23	57	13.2	6.1	5.1	20.8	0.5	8.3	8.4	110
16	33	311	383	8.57	29	18.8	4.1	8.6	47.8	0.5	5.9	41	185
21	33.2	310	311	8.43	78	22.1	4.8	10.4	40.2	0.3	5.3	4.6	223
Group 2 (Xolotlan Lake)													
1	29.5	1434	n.m	8.86	136	378	59.7	19.7	22.6	0.9	227	54.8	671
2	28.7	1365	n.m	8.81	23	350	49.2	19.1	22.7	1.1	217	57.3	649
3	28.7	1334	n.m	8.87	14	348	40.5	20.3	24.3	0.9	223	56.5	620
4	29.9	1421	n.m	8.93	38	391	57.3	20.7	23.9	0.9	225	55.3	647
5	29.3	1316	1795	8.92	26	346	43.8	15.3	13.4	0.9	208	55.6	633
6	29.7	1245	1575	8.92	36	340	41.5	25.2	35.1	0.9	195	46.5	561
8	30.5	1408	1792	8.91	30	394	51.0	19.9	13.7	0.9	232	54.0	642
12\1	28	765	n.m	8.66	76	153	29.7	13.3	23.9	0.8	51.5	39.9	453
20	28.4	1351	1640	8.60	27	346	54.4	19.1	24.2	0.9	222	58.8	627
22 (12)	31.1	707	n.m	8.29	46	141	17.1	12.7	45.8	0.6	135	49.9	305
Group 2													
30	31.6	163	88	9.39	95	21.3	7.8	3.2	17.6	0.3	12.6	5.5	95
31	29.7	210	95	7.62	200	13.4	11.1	6.0	28.9	0.5	19.6	2.3	128
40	31	1242	1335	7.95	103	217.4	34.3	72	48.0	1.4	166	444	259
45	29.5	166	120	8.09	131	13.8	3.1	3.4	25.0	0.2	11.0	9.0	101
49	30	374	531	8.25	n.m	70.8	18	8.8	18.4	0.4	53.9	39.0	165
65	29.6	362	372	8.69	37	51.9	14.8	14.2	12.3	0.3	10.1	2.5	256
81	29.5	350	417	8.37	90	61.5	15.4	6.4	20.6	0.5	52.6	25.2	168
82	n.m	340	198	8.56	46	61.4	15.3	6.4	20.6	0.5	52.3	25.2	159
83	n.m	382	198	7.30	−32	59.4	15	6.4	30.4	0.5	46.2	35.1	189
84	n.m	383	424	7.39	−51	59.6	15	6.3	30.7	0.5	46.8	35.4	189
85	n.m	403	166	7.36	−61	64.0	15.4	8.3	30.1	0.6	46.5	37.3	201
Group 3													
18-1	31.9	4876	6700	8.21	25	1440	166	77.9	80.7	13.0	2339	319	441
44	31.8	1513	1360	8.52	50	239	64	103	21.7	0.3	239	76.5	770
46	30	4997	5440	8.73	47	1536	118	95.8	22.1	0.6	2135	39.4	1051
52	29.8	4180	3870	8.02	49	1234	139	66.9	63.7	0.9	2087	254	336
53	29.2	4377	3720	7.78	77	1283	147	69.8	87.5	1.0	2109	332	348
54	29	4447	3500	7.13	−30	1318	147	71.3	78.9	0.9	2083	330	418
55	29	4291	4030	7.08	50	1243	142	68.0	77.2	1.0	2088	260	412
64	29.5	2983	3310	8.01	70	847	134	29.2	77.0	1.0	1377	295	223
Group 4													
17	47.6	1356	2230	6.74	102	185	40	72.1	111	0.5	191	279	477
32	30.1	364	151	7.03	193	30.6	5.7	11.5	47.3	0.1	14.0	11.3	244
35	34	354	348	7.36	107	56.3	6.3	3.6	35.4	0.2	10.8	28.4	214

36	28	340	360	6.75	68	24.5	2.3	10.8	48.0	0.2	7.7	5.3	241
37	28	159	150	6.64	220	10.6	5.5	4.0	25.7	0.5	3.3	3.2	107
39	29	620	845	6.90	140	27.5	6.8	48.6	154	0.3	81.0	34.2	268
41	47	1220	1320	6.63	210	168	30.3	60.4	96.4	0.2	191	262	412
42	45	970	1050	6.38	146	149	25.8	39.6	62.2	0.3	81	209	404
43	41	1188	1400	6.76	82	189	34.5	58.4	115	0.9	225	252	313
47	30.2	443	52	7.45	102	38.5	7.5	17.9	47.6	0.6	8.1	13.3	310
48	25.8	375	335	7.74	64	35.2	5.4	23.7	44.3	0.3	50.1	33.2	183
57	37	464	440	7.39	33	36.5	6.7	18.3	52.5	0.5	4.2	73.4	272
60	33.7	742	890	7.41	63	135	15.8	18	45.6	0.3	179	27.2	320
61	29	545	583	7.08	102	39.4	7.1	30.9	57.7	0.3	7.8	11.7	390
62	29.5	434	545	7.04	101	40.3	5.8	21.9	43.4	0.2	15.6	23.1	284
66	28.5	400	415	7.17	638	45.0	10.5	11.6	41.5	0.3	31.9	36.8	223
67	28.5	341	217	7.41	250	24.1	8.8	15.6	40.8	0.4	22.1	24.4	204
68	28.3	356	365	7.77	586	54.6	14.5	6.5	27.9	0.4	30.3	29.9	192
69	29.1	327	343	7.68	162	51.4	12.4	5.1	24.4	0.4	25.2	25.1	183
70	29.5	313	327	7.63	141	49.8	12.8	4.9	23.6	0.6	26.0	30.3	165
71	33	414	403	7.15	106	47.3	12.6	9.5	43.8	0.3	23.8	32.5	244
72	31	408	421	7.29	130	44.8	14.9	9.3	43.4	0.2	21.9	20.3	253
73	30.6	452	426	7.23	110	49.4	16.6	15.0	46.3	0.2	33.3	22.4	268
74	31.2	408	439	7.29	107	49.1	16.0	8.8	41.7	0.3	28.4	28.6	235
75	35.2	409	394	7.62	93	89.0	12.8	3.3	15.8	0.4	30.7	37.2	220
76	30.2	385	406	7.45	123	48.6	15.2	7.0	40.1	0.4	26.7	30.9	217
77	25.6	303	287	7.37	470	23.7	8.7	9.5	37.3	0.7	15.7	18.3	189
78	27.2	305	313	7.61	176	41.6	12.1	5.4	27.5	0.7	22.2	27.5	168
79	27.3	303	293	7.50	136	36.4	12.4	6.9	28.1	0.7	20.0	24.5	174
80	28.2	340	347	7.69	148	63	12.3	6.4	19.9	0.7	30.1	33.6	174
86	30.3	878	948	6.98	121	184.8	13.4	21.8	55.0	0.6	157	186	259
87	27.2	570	519	7.48	125	95.5	13.7	10.5	36.5	0.6	37.2	34.0	342
88	29.7	392	402	7.75	100	86.4	9.0	4.4	13.1	0.7	30.7	36.8	210
89	31.5	405	410	7.03	136	34.0	9.8	13.0	48.1	0.2	13.3	11.9	275
90	26.8	311	319	7.40	179	28.7	9.6	11.1	31.4	0.1	6.4	4.2	220
91	27.2	244	225	7.59	137	19.9	8.0	8.6	22.4	0.1	1.8	0.6	183
92	26.9	259	218	7.63	137	27.8	9.0	6.7	22.0	0.1	2.9	0.8	189
93	30.4	508	418	7.72	121	90.0	16.6	13.9	16.7	0.4	18.6	10.1	342
94	37.2	1178	1305	7.01	203	266	18.2	20.0	75	0.4	213	289	296
Group 5													
14	86	1288	2960	8.43	−210	246	6.6	0.3	153.6	2.2	100	724	54.9
33	43.5	855	846	8.13	−35	177	3.0	0.6	75.5	1.2	78	463	58.0
34	37.5	929	120	8.09	119	202	4.2	0.2	84.9	1.1	76	512	48.8
38	42	1501	1290	7.52	110	265	8.9	0.97	189	2.2	77	849	110
59	38	1523	2020	7.20	58	404	18.4	15.4	64.9	0.7	240	412	368
63	36	4959	4240	6.88	77	1367	149	17.4	182	2.4	1213	1673	355

(*continued on next page*)

Table 1 (*continued*)

Samples	*T* (°C)	TDS (mg/l)	Cond (μS)	pH	Eh	Na (mg/l)	K (mg/l)	Mg (mg/l)	Ca (mg/l)	F (mg/l)	Cl (mg/l)	SO_4 (mg/l)	HCO_3 (mg/l)
Group 6													
18t/1	55	6308	3880	5.66	−258	1213	125	138	143	13.2	2226	1949	500
18/t2	48	4342	9250	6.02	−300	1280	104	79.4	128	3.7	1950	324	473
9bis	39.1	7026	1916	8.38	35	2385	302	0.5	27.2	5.2	3459	127	720
11	93	1007	n.m	7.60	−360	311	15.5	0.8	25.9	1.7	296	183	172
50	100	3918	5440	8.40	−30	1302	175	<0.3	46.5	1.5	2135	185	73.2
51	100	3853	5440	8.12	−121	1276	193	<0.3	23.9	1.5	2221	80	58.0
56	47	3901	3300	6.01	−255	1136	94	62.4	123	0.5	1941	122	421
58	36	4506	5330	8.52	−65	1355	153	70.2	78.6	0.9	2168	345	336

n.m.: not measured.

re-established as a result of the hurricane Mitch, which caused the level of the lake to rise by 4 m. The lake gathers approximately 0.3–0.7 km^3/year of water from rivers and about 0.9 km^3/year from rainwater, in addition to inflow from the groundwater system. The potential evaporation has been estimated at 1990–2050 mm/a by Reyes García (1977). More recently, Rozanski (1999) showed that groundwater constitutes the greatest inflow to the lake (~1.850 hm^3/a). Evaporation and outflow account for the greatest loss, ~900 hm^3/a.

Groundwater in the Managua area flows within a 400–600 m-thick succession of semi-consolidated, permeable pyroclastic deposits of Pleistocene age, overlain by a thin layer of alluvium and colluvium of Pleistocene–Oligocene age. The most productive aquifers, utilized by wells with a flow of up to 80 l/s, are located near the main active volcanic structures, where the highest permeability is expected.

The volcanic lake "Asososca de Mananagua", housing the municipal waterworks, situated about 2 km from the Managua lake, has a diameter of 1 km, a maximum depth between 90 and 100 m and a water volume estimated at 4000 m^3. It has been used since 1930 and it constitutes about 25% of the water supply of Managua. The rest is supplied by several municipal wells. Due to an increasing demand for water, the extraction increased from 3.8×10^4 m^3/day in 1930s to ~10^5 m^3/day in the 1990s.

2.3. Sample description, sampling and analytical techniques

This study reports compositional data for 85 surface water and groundwater samples, collected during two field campaigns in June 2002 and July 2003, respectively. They include: 10 samples from Lake Xolotlan (Managua), a large shallow-water basin subject to considerable pollution; 18 volcanic lakes (small volcanic lakes: Jiloa, Apoyeque, Asososca de Leon, and Asososca de Managua, Tiscapa, Nejapa, Apoyo, Monte Galan, Masaya); 4 rivers, 3 production wells from the Momotombo geothermal plant; 10 thermal waters; 40 groundwater samples from Managua city and district, from Chiltepe peninsula and from the Momotombo area, collected from 18 private wells and 22 ENACAL (municipal waterworks of Managua) wells. The location of sampling points is shown in Fig. 1. In the following discussion, the collected waters are divided into 6

Table 2
Minor and trace elements determination by ICP-MS for selected samples

Samples no.	Li	B	Al	V	Cr	Mn	Fe	Co	Ni	Cu	Zn	As	Se	Rb	Sr	Cd	Sb	Ba	Tl	Pb	U
	(μg/l)	(μg/l)	(μg/l)	(μg/l)	(μg/l)	(μg/l)	(μg/l)	(μg/l)	(μg/l)	(μg/l)	(μg/l)	(μg/l)	(μg/l)	(μg/l)	(μg/l)	(μg/l)	(μg/l)	(μg/l)	(μg/l)	(μg/l)	(μg/l)
Group 1 rivers																					
15	1.1	141	142	11.5	0.01	11.1	73.5	0.11	3.91	3.94	6.86	3.71	0.70	5.34	152	0.38	0.15	76.9	0.02	0.94	0.1
16	n.d	64	77	8.2	0.02	28.4	71.1	0.01	2.51	0.62	3.24	8.63	0.52	1.90	260	0.02	0.22	89.0	0.01	0.36	0.13
21	4.0	142	160	18.0	0.02	6.79	91.9	0.19	31.5	3.81	4.23	2.30	0.88	4.88	306	0.12	0.09	191	0.02	1.02	0.19
Group 2 (Lake)																					
4	8.5	2020	50.6	60.5	0.05	0.93	33.5	0.07	40.9	10.5	5.39	31.8	1.78	22.0	244	0.03	0.8	132	0.01	0.59	1.47
5	8.2	2030	98.5	61.7	0.09	1.35	57.4	0.1	44.3	11.4	10.2	31.3	1.65	21.8	243	0.04	0.83	136	0.01	1.05	1.49
6	6.3	1650	51.5	57.0	0.09	0.42	33.0	0.08	27.3	8.72	2.90	28.1	1.92	18.9	237	0.08	0.75	132	0.02	0.54	1.32
8	7.6	2050	73.3	60.5	0.05	0.91	59.5	0.09	29.7	9.51	5.78	31.5	1.82	21.7	243	0.38	0.82	138	0.01	1.01	1.5
20	7.7	1960	67.6	72.0	0.04	1.31	45.3	0.19	23.3	8.87	5.45	28.2	2.08	20.5	237	0.06	0.95	124	0.01	1.21	1.59
22 (12)	12.7	1130	2080	63.1	0.08	12.6	302	0.33	18.6	26.4	44.2	24.7	1.29	14.3	273	0.33	0.76	148	0.02	5.42	1.39
Group 2																					
30	0.33	46.2	11.8	18.8	0.17	1.96	6.13	0.44	0.60	1.23	1.01	1.81	0.16	5.89	68.8	0.01	0.45	7.33	1.29	0.93	2.18
31	0.04	38.0	12.7	16.2	0.11	4.50	11.54	0.22	0.97	2.97	0.15	0.85	0.39	5.75	129	0.01	0.28	56.9	1.29	0.93	2.39
40	60.4	996	9.82	4.8	0.24	20.0	22.4	n.d	2.04	2.74	1.47	15.3	0.76	49.2	468	n.d	n.d	105	2.58	1.89	4.28
45	0.20	33.9	67.9	20.2	0.43	93.1	326	0.36	4.28	7.75	8.36	1.78	0.20	2.49	153	0.04	0.11	76.9	1.3	1.69	2.13
49	1.69	77.0	0.57	184	0.76	0.09	2.54	0.02	0.58	0.82	n.d	4.38	0.87	8.05	114	0.01	0.97	19.2	1.29	0.89	2.89
65	1.67	115	15.7	6.2	0.10	2.79	9.37	n.d	0.82	1.28	0.90	0.60	0.15	11.7	87.5	n.d	n.d	17.1	1.29	0.92	2.14
81	4.07	93.1	4.33	161	2.24	2.16	10.0	1.93	0.55	1.58	n.d	5.71	1.66	11.1	135	n.d	n.d	21.0	1.3	0.92	2.94
85	4.02	98.9	2.98	135	2.09	31.9	14.5	1.96	1.06	1.40	n.d	6.15	0.73	10.9	145	n.d	n.d	23.7	1.32	0.93	2.83
Group 3																					
18\1	1930	n.d	375	19.8	n.d	32.4	262	0.05	22.1	21.6	151	590	n.d	490	1200	0.44	22.2	283	0.11	49.1	0.97
44	21.2	4600	4.58	12.3	0.21	6.08	8.74	n.d	0.70	2.78	0.24	68	1.15	80.8	60.8	n.d	n.d	48.0	2.58	1.82	4.96
46	1625	16002	5.59	15.8	1.00	44	13.5	0.09	0.77	17.9	n.d	39.2	9.40	207	122	0.00	0.26	125	12.9	8.94	20.1
52	1830	19500	11.3	50.6	1.10	0.47	20.8	0.15	2.73	15	n.d	622	8.40	414	940	0.01	18.1	222	12.9	8.96	20.9
53	1880	20300	11.4	49.4	1.14	2.39	21.8	0.15	3.03	14.8	n.d	716	9.18	417	1020	0.03	18.3	226	12.9	8.89	20.9
54	1880	20000	10	48.4	1.07	12.8	21.1	0.15	2.94	14.3	n.d	650	8.55	418	1020	0.02	18.2	230	12.9	8.89	20.9
55	1890	20500	7.57	47.1	1.15	13.3	19.4	0.15	3.02	14.6	n.d	723	9.13	419	1030	0.03	18.4	231	12.9	8.89	20.9
64	525	4945	2.91	28.1	0.44	0.70	8.95	0.06	1.27	5.05	n.d	120	2.67	188	430	0.00	3.29	84.0	6.6	4.44	10.15
Group 4																					
17	118	n.d	14.4	39.4	n.d	1.54	n.d	n.d	n.d	n.d	n.d	107	1.65	57.1	552	n.d	0.15	105	0.03	n.d	0.71
32	1.7	26.6	3.46	136	0.99	0.53	18.4	n.d	2.55	1.00	16.5	2.56	1.55	3.65	192	n.d	n.d	86.7	1.29	1.07	2.69
35	4.9	81.8	2.23	116	0.50	0.27	7.6	0.04	1.01	0.84	15.4	4.96	0.28	14.3	170	0.01	0.08	43.2	1.29	1.02	2.3
36	2.5	21.5	2.55	73.9	0.38	11.1	10.1	0.08	1.51	0.54	3.0	2.93	0.10	1.38	211	0.01	0.09	45.8	1.29	0.93	2.62
37	1.7	13.0	2.93	40.0	0.23	1.07	9.03	n.d	1.14	0.27	1.4	1.10	0.14	2.23	111	n.d	n.d	42.9	1.29	0.91	2.03
39	3.9	19.3	2.85	89.8	0.54	1.94	67.6	0.21	8.74	0.51	18.1	2.31	0.82	5.98	847	n.d	n.d	328	1.2	0.91	2.81

(*continued on next page*)

Table 2 (*continued*)

Samples no.	Li	B	Al	V	Cr	Mn	Fe	Co	Ni	Cu	Zn	As	Se	Rb	Sr	Cd	Sb	Ba	Tl	Pb	U
	(μg/l)	(μg/l)	(μg/l)	(μg/l)	(μg/l)	(μg/l)	(μg/l)	(μg/l)	(μg/l)	(μg/l)	(μg/l)	(μg/l)	(μg/l)	(μg/l)	(μg/l)	(μg/l)	(μg/l)	(μg/l)	(μg/l)	(μg/l)	(μg/l)
41	108	2200	7.18	50.4	0.38	0.21	30.8	n.d	4.04	2.18	0.49	120	1.63	52.4	450	n.d	n.d	95.2	2.6	1.81	4.7
42	108	2073	7.16	48.8	0.34	0.33	21.7	n.d	3.11	6.40	1.00	116	1.79	43.1	301	n.d	n.d	68.4	1.3	0.91	2.46
43	35.4	1852	35.2	55.8	0.53	5.24	48.2	n.d	5.38	2.40	2.08	105	3.94	50.4	450	n.d	n.d	128	2.6	1.92	4.86
47	8.9	32.4	7.29	143	0.79	1.86	25.9	n.d	3	1.42	10.5	3.94	3.26	3.83	225	n.d	n.d	102	1.29	0.96	2.56
48	3.9	21.6	7.71	53.1	0.69	1.70	37.2	n.d	2.49	1.66	40.2	2.31	2.55	3.53	137	n.d	n.d	18.8	1.29	0.97	2.42
57	3.6	45.8	6.76	15.1	0.73	8.68	16.6	0.08	1.82	1.12	1.44	13.8	0.29	2.28	94.8	0.01	0.06	12.7	1.29	0.92	2.13
60	52.5	647	3.74	21.8	1.42	0.77	14.4	0.06	1.43	1.66	26.7	12.6	1.14	15.7	196	0.01	0.1	91.5	1.3	0.97	2.37
86	51.3	588	4.98	27.2	0.25	15.9	66.4	0.09	2.67	3.63	187	6.38	6.40	9.30	157	n.d	n.d	31.3	1.29	0.9	3.28
89	7.3	113.2	5.54	113.2	2.29	2.39	22.4	2.28	2.83	2.32	0.97	6.09	1.34	8.90	297	n.d	0.84	57.0	1.63	1.41	3.79
91	1.8	29.6	5.36	227	0.93	0.28	12.7	n.d	1.45	2.65	1.82	4.90	0.34	7.94	74.9	n.d	n.d	28.5	1.29	1.9	2.5
92	1.0	34.2	8.07	265	1.11	0.18	14.3	n.d	1.39	0.85	2.18	2.98	0.38	3.94	74.2	n.d	n.d	25.8	1.29	0.93	2.53
93	19.7	371	8.86	28.5	0.22	0.71	12.7	n.d	1.05	8.29	8.12	1.79	0.31	15.1	65.3	n.d	n.d	11.7	1.3	1.25	2.21
94	77.0	1180	2.46	32.6	0.34	1.63	31.8	0.1	2.76	3.22	101	2.20	2.70	19.2	140	0.02	0.05	38.8	2.58	1.94	4.98
Group 5																					
14	317	n.d	186	1.52	n.d	77.4	95.7	n.d	48.6	28.4	287	75.5	n.d	54.2	1220	0.93	1.46	66.5	0.09	2.13	0.09
33	49.7	523	7.63	1.37	0.09	6.34	18.9	0.11	2.68	2.08	1.11	21.2	0.28	3.39	259	0.02	0.07	9.57	1.29	0.92	2.01
34	50.7	517	3.8	1.57	0.11	1.89	16.7	0.11	2.66	2.13	0.76	20.0	0.30	3.50	262	0.02	0.08	8.64	1.29	0.92	2.01
38	77.8	858	10.5	10.0	0.23	0.84	54.8	0.27	7.12	3	2.10	21.4	0.52	12.5	1194	0.04	0.39	40	2.58	1.82	4.16
59	74.8	1418	5.72	45.8	0.40	0.52	20.6	n.d	2.40	4.44	3.88	21.8	5.26	15.9	266	n.d	n.d	32.4	2.58	1.8	5.58
Group 6																					
18t/1	1460	n.d	127	1.7	n.d	926	8530.0	n.d	22.2	11.3	44.4	184	n.d	201	1450	3.34	2.88	132	0.12	3.22	0.07
18/t2	1310	n.d	39.5	n.d	n.d	386	n.d	n.d	5.41	7.91	22.8	17.4	n.d	188	1540	0.17	0.22	320	n.d	n.d	0.07
9bis	8530	n.d	486	n.d	n.d	24.3	68.5	n.d	22.2	16.6	13.8	2650	n.d	1750	418	0.20	176	85.6	10.3	0.49	0.02
11	358	n.d	122	n.d	n.d	51.3	262	n.d	16.9	4.21	177	150	n.d	58.6	352	0.94	2.4	25.6	0.31	14.2	0.02
50	3080	16240	175	18.7	1.57	4.98	51.2	0.12	2.56	14.6	n.d	1876	9.6	662	758	0.07	70.6	52	29.2	17.8	40
51	3300	16040	290	15.9	2.14	6.48	79.8	0.21	6.24	15.3	n.d	1744	9.3	810	280	0.06	628	13.6	51.8	18.3	40
56	1350	17300	13.8	17.0	1.04	401	644	0.35	4.73	13.1	n.d	21.4	7.7	188	1287	0.01	0.37	366	12.9	8.93	20.1
58	940	10500	21.5	27.7	0.63	62	23.0	0.21	1.43	8.15	n.d	269	4.9	208	520	0.02	7.70	172	6.45	4.46	10.6

n.d.: not determinated.

different main groups. These include 3 types of surface waters: Group 1, river waters; Group 2, lake waters with TDS < 1500; Group 3, lake waters with TDS > 1500; and 3 types of groundwaters, divided on the basis of the prevalent ionic species: Group 4, HCO_3 groundwaters; Group 5, SO_4 groundwaters; Group 6, Cl groundwaters. In the above grouping, contrasting compositions and/or total dissolved salts are assumed to reflect different source processes.

Temperature, pH and Eh were measured directly in the field with portable instruments. Samples were collected and stored in PE bottles. An aliquot for cation analysis was filtered (0.45 μm MF Millipore filters) and acidified with HNO_3. Chloride, NO_3, SO_4, Na, K, Ca and Mg contents were determined on a DIONEX DX-120 ion chromatograph, while minor and trace elements were analysed with an ELAN-DRCe ICP-MS (Inductively Coupled Plasma – Mass Spectrometer). Analytical results are reported in Tables 1 and 2. The aqueous speciation of dissolved chemicals and saturation indices for the most relevant mineral phases were computed using the PHREEQC code (version 1.4 for Windows; Parkhurst, 1995; Parkhurst and Appelo, 1999) and the WATEQ4F supporting thermochemical database (Ball and Nordstrom, 1991).

3. Results and discussion

3.1. Main hydrogeochemical features

3.1.1. Surface waters

The temperature of river waters (Group 1; crosses in Fig. 2) are close to ambient (31–33 °C), total dissolved salts typically ~300 mg/l, and Eh values 30–80 mV, reflecting O_2 consumption of decaying organic matter. They typically display a HCO_3-alkaline-earth composition. Lakes (Groups 2 and 3) have a bimodal distribution of total dissolved salts, with a threshold at TDS ~ 1500 mg/l. In the first group, salinities as low as ~1635 mg/l (site 30) reflect a predominant meteoric contribution, also supported by HCO_3^- being the main anion species. In terms of cation content, Group 2 surface waters range from Ca-dominated to alkali-rich (Fig. 2). The higher total dissolved salt content of Group 3 volcanic lakes (TDS between 1513 and 4997; Table 1) is also paralleled by a drift toward predominant Na–Cl compositions (Table 1 and Fig. 2), suggestive of the occurrence of more complex geochemical processes, either (i) more extensive

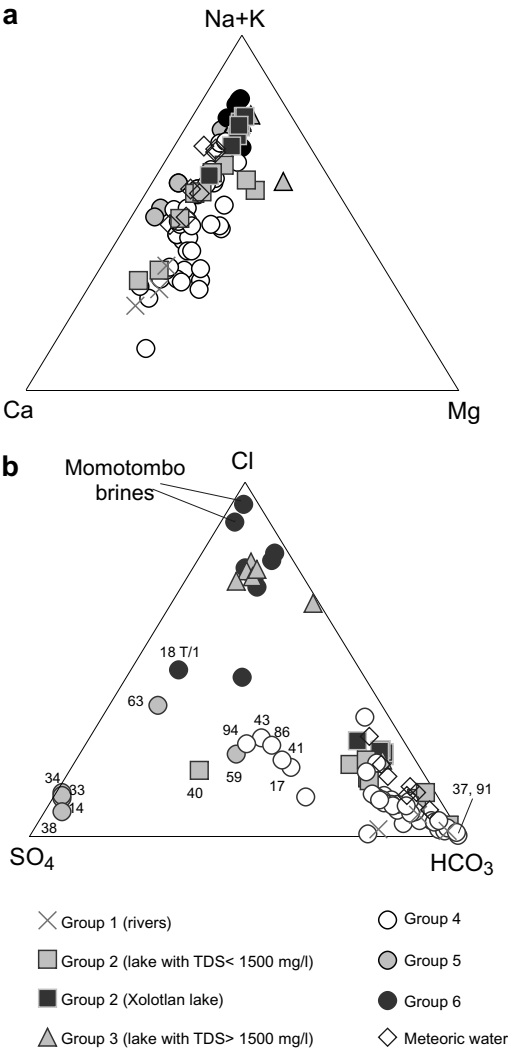

Fig. 2. Triangular diagrams of major anions (a) and cations (b). Waters are subdivided into 6 groups as in Table 1. Meteoric water samples from Parello (unpublished data).

evaporation within a closed basin exclusively fed by rainwater or (ii) more likely, underground recharge from saline groundwaters (see below). As regards process (i), in order to alter the composition of the lake by evaporation, from HCO_3 -dominated to Cl-dominated compositions, super-saturation for a carbonate mineral phase (and thus calcite precipitation in the lake-bottom sediments) is required, as supported by calculated saturation indices (Fig. 3a). It is however interesting to note that the saline (Group 3) lakes are located within recently-formed volcano-hosted depressions or calderas (e.g., Apoyeque, Jiloa, Apoyo) and that thermal manifestations (fumarolic gas emanations, thermal

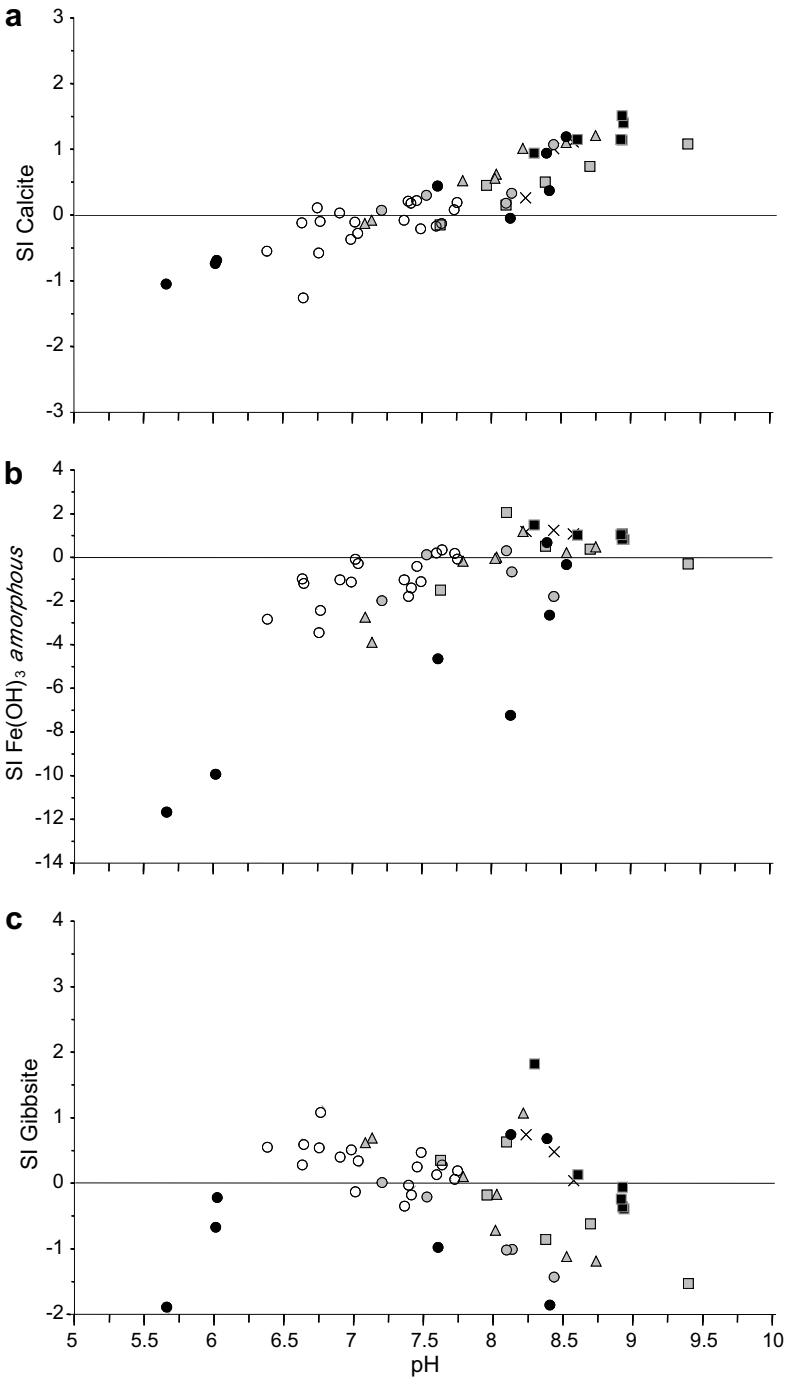

Fig. 3. SI (saturation index) versus pH binary diagrams for some secondary minerals (a: calcite; b: $Fe(OH)_3$ amorphous; c: gibbsite). SI values are calculated by means of the PHREEQC software (Parkhurst, 1995) using the Wateq4f.dat thermodynamic database. Symbols as in Fig. 2.

springs) are common on the lakes' shores, springs having a composition similar to that of the neighbour lakes (see Group 6 groundwaters). Thus, it is suggested that process (ii) is more likely to be the key factor controlling the composition of saline (Group 3) lakes (cf. 3.2). As for Group 2, pH ranges from neutral to basic, but redox conditions are typically more reducing (Eh between −30 and 77 mV).

3.1.2. Groundwaters

The temperature of most of the HCO_3-dominated (Group 4) groundwaters is between 25 and 35 °C, TDS < 500 mg/l, and pH slightly acid to neutral (6.4–7.8), all suggesting a relatively shallow and fast underground circulation within the aquifers. They are thus likely to be representative of the meteoric component in the area, modified by low-temperature leaching of the host volcanic rocks. Only a few acidic samples (17, 41–43), collected, between the Monte Galan Caldera and Asososca de Leon volcano (near the Momotombo volcano), characterized by higher salinities (up to 1356 mg/l) and temperatures (up 50 °C), reflect more extensive gas–water–rock interaction as a consequence of deeper/longer circulation paths. The geothermal character of the SO_4-rich (Group 5) groundwaters is supported by temperatures in the range 36–86°C, TDS up to ~5 g/l and recurrent reducing conditions (Eh as low as −210 mV in site 14). Some of these samples were drawn from wells along active tectonic lines, like the Punta Huete fault (38) or the NS fault in the Chiltepe peninsula (59), others from springs in the NE sector of the area being studied, near *Las Canoas* lake (33, 34). On the other hand sample 63 was collected from a steaming pool on the Apoyo volcanic lake shore. Sodium, and subordinately Ca, are the main cation species, while Mg contents are anomalously low (as low as 0.3 mg/l). In the triangular diagram of Giggenbach (1988) (Fig. 4), most Group 5 samples plot in the field of partially equilibrated waters (e.g., samples 33, 34, 38), implying that the low Mg contents reflect deep water–rock equilibration at temperatures in the range 120-240 °C (based on the Na/K solute geothermometer; Giggenbach, 1988), followed by minor re-equilibration (and Mg-uptake) at discharge conditions. Finally, Na–Cl groundwaters (Group 6) are found in the Chiltepe peninsula near Jiloa lake (samples $18t_1$, $18t_2$, 56 and 58), in the Momotombo area and in the Tipitapa area (sample11). They have high TDS (1–6.3 g/l), high temperatures (36–93 °C), and compositions more or less similar to liquid samples extracted from the Momotombo geothermal plant (samples 9bis, 50 and 51). The temperatures of the thermal springs on Jiloa lake shore are between 47 and 55 °C, TDS between 3901 and 6308 mg/l, pH between 5.7 and 8.5 and strongly reducing Eh-values (as low as −300 mV). Both low pH and Eh from these springs (which manifest themselves at the surface as small bubbling pools) reflect the interaction with CO_2 and H_2S-rich hydrothermal steam, feeding the nearby fumaroles. In the triangular plot of Fig. 4, fluids extracted from the Momotombo geothermal plant plot on the full-equilibrium curve of Giggenbach (1988) at ~260–280 °C, in reasonable agreement with temperatures measured at well-bottom (230–270 °C); on the other hand, most thermal

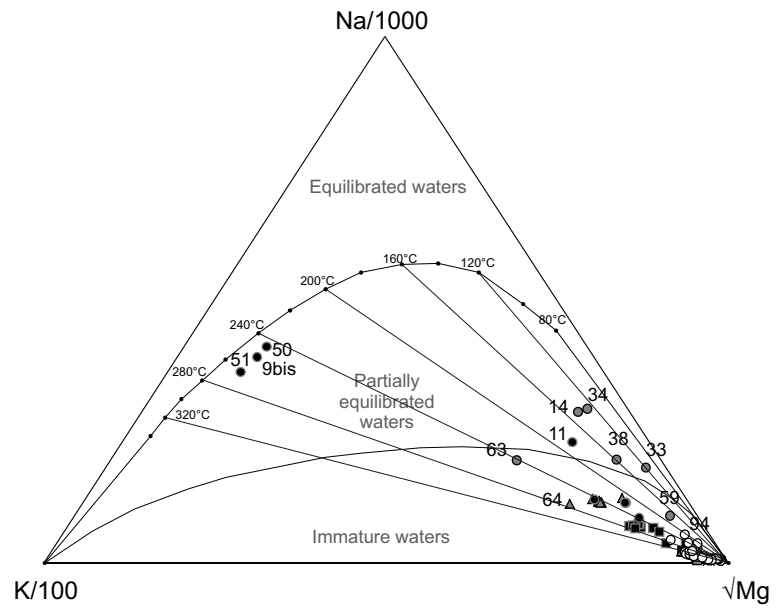

Fig. 4. Na, K, Mg triangular geo-indicator diagram (Giggenbach, 1988) for all sample groups; water–rock equilibration temperatures are based on Na/K solute geothermometer (Giggenbach, 1988).

springs on the Jiloa lake shore fall within the field of immature waters, suggesting the occurrence of near-surface, gas–water–rock interaction upon discharge and dilution with meteoric and/or lake waters.

3.2. Mixing relations between different end-member compositions

The triangular diagrams in Fig. 2 reveal potential relations between different water types. A more or less continuous compositional trend, from Ca-rich (Group 1) rivers to Na-rich (Group 6) groundwaters is seen in Fig. 2a; more diverse compositions are observed in Fig. 2b, with at least 3 compositional end-members: (a) geothermal well waters from the Momotombo plant, representative of the Cl-rich end-member; (b) samples 14, 33, 34 and 38 (Group 5 groundwaters), clustering near the SO_4 corner; (c) samples 37 and 91, clustering close to the HCO_3 corner and being, among HCO_3 groundwaters, those probably most representative of recent meteoric recharge. While low salinity volcanic lakes, rivers and most groundwaters of the ENACAL network plot close to the HCO_3 corner, more or less conforming with the composition of end-member (c), a large number of samples plot in intermediate positions between the above-mentioned end-members in Fig. 2B. Group 3 saline volcanic lakes (Apoyeque, Jiloa) and the saline (Group 6) thermal waters discharging along the lake's shore tend to plot close to Momotombo well water, except samples 63 and 18 t_1 (two thermal springs along the shores of the Apoyo and Jiloa volcanic lakes, respectively), which are typically displaced toward the SO_4 corner. The sample from *Monte Galan* lake (40) and a large number of groundwater samples, collected within the Chiltepe Peninsula (59, 86, 94) and in the Momotombo area (17, 41, 42, 43), plot in the central portion of the diagram, showing a relative enrichment in Cl and SO_4 relative to the main cluster of the HCO_3-rich groundwaters.

In very general terms, these intermediate compositions are suggestive of mixing processes between different water types, and this hypothesis is tested in the Na vs. Cl scatter diagram of Fig. 5a. Examination of the same diagram suggests that most compositional variability in the dataset can be ascribed to binary mixing (see mixing lines AT and A′T in the diagram) between dilute HCO_3 groundwaters (whose compositional range is typified by samples 37 and 91) and an NaCl-brine component (whose composition is fixed by fluids from Momotombo geothermal field). The above-mentioned HCO_3 groundwaters have Cl and SO_4 concentrations similar to local rainwater (Fig. 5a–c), while displaying some cation excess; they are thus representative of shallow-infiltrating meteoric waters that have experienced minor cation leaching from the aquifer host rocks. Examination of Fig. 5a also suggests that the proportion of the NaCl-brine component in the mixture is significant (30–70%) in Group 6 thermal groundwaters and, even more importantly, in the saline volcanic lakes Apoyeque and Jiloa. The latter thus appear to be fed in large part by the underground discharge of thermal fluids, while generally containing minor($<2\%$) amounts of HCO_3 groundwater and Group 2 (dilute) volcanic lake components, with the exception of samples plotting in the middle section of Fig. 2a, as described above (40, Monte Galan lake; 59, 86, 94, Chiltepe Peninsula; 17, 41, 42, 43, Momotombo area).

While the above-mentioned mixing process appears widespread in the study area, and decisive in controlling the chemistry of most fluids analysed, it does not account for the composition of Group 5 groundwaters and of the Xolotlan (Managua) lake, which are richer in Na than mixing lines 1 and 2 would explain. Similar considerations are suggested in Figs. 5b–c, in which the Cl concentration is contrasted with SO_4 and total dissolved solute concentration, respectively.

Two additional processes can be envisaged for the evolution of Group 5 groundwaters and Xolotlan lake water: (i) low temperature leaching of the host rocks; and (ii) evaporation. Process (i) was quantitatively evaluated by calculating the model compositions of waters formed by irreversible stoichiometric dissolution of volcanites from the Las Sierreas formation (whose composition was computed by averaging whole rock and matrix analyses of volcanic rocks from the study area; this study and Wehrmann, 2005). The model line representing the rock-leaching process (obtained by step-wise addition of increasing amounts of rock to average rainwater composition, see line labelled "*rock leaching*" in Fig. 5a) nicely reproduces the compositional shift from rainwater to dilute HCO_3 groundwaters (e.g., sample 37); however, it does not fit the analysed composition of Group 5 and Xolotlan lake waters, suggesting that either rock leaching is not stoichiometric (e.g., that Na is retained in the solid in preference to Cl), or that process (i) is not playing a decisive role in the maturation of the fluids analysed. On the other hand, the "evaporation lines" drawn in Figs. 5a and b highlight

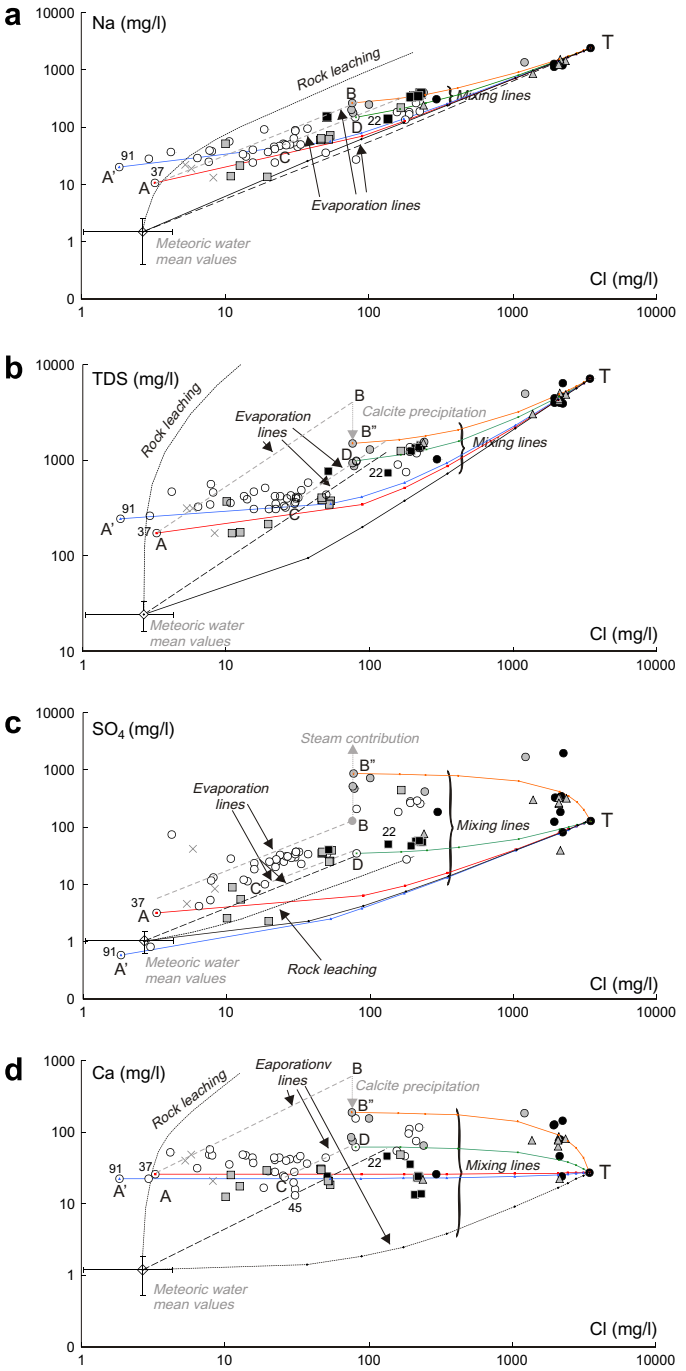

Fig. 5. Scatter diagrams plotting Na (a), TDS (b), SO_4 (c), Ca (d) versus Cl for the different water types. The coloured lines represent the mixing trends between a NaCl-brine (thermal end-member) and a HCO_3-water (red and blue lines) or SO_4 -groundwaters (green and orange lines), respectively; while the dark line shows the mixing trends with a mean of meteoric water samples (Parello, unpublished data). The black dotted line is the model path representing the rock-leaching process of the host volcanic formation operated by meteoric water. Cation contents of the HCO_3-water samples, used for modelling the above mentioned mixing trend lines (wells 37 and 91), are consistent with being derived from stoichiometric leaching of 500 g of rock (per 1000 l of solution) by shallow infiltrating meteoric waters. Grey dashed lines describe the evaporation process of HCO_3-water representing the meteoric end member. In (b) and (d) B–B″ line represents the calcite precipitation (for details see the text). T = thermal end-member. Symbols as in Fig. 2.

the fact that evaporation of HCO_3 (meteoric-derived) groundwaters are a plausible source for the Group 5 samples. It is proposed that evaporation takes place through heating by the CO_2^- and H_2S-bearing, hydrothermal vapours bubbling into these stagnant pools; as also supported by the high temperatures, the prevailing reducing and acidic conditions and high SO_4 concentrations (from oxidation of H_2S; see Fig. 5c). The composition of Xolotlan Lake can in turn be explained in terms of evaporation of HCO_3 meteoric components (lines A–B and/or C–D) followed by mixing (~2%) with the geothermal end-member (mixing lines B″–T and D–T). This hypothesis is consistent with the results of hydrological balance calculations, which suggest that groundwater inflow and evaporation are the main input and output in the Xolotlan Lake (Rozanski, 1999). The inflowing groundwaters are to a minor extent saline, and a geothermal characteristic is not evident from geological observations, but it is not surprising since the lake is located inside a main volcano-tectonic depression and is surrounded by active volcanic and thermal areas. Variables such as TDS (Fig. 5b) and Ca (Fig. 5d) suggest an open system, e.g., the vertical distance between B and B″ in Fig. 5d can be ascribed to calcite precipitation during the evaporation process, calcite being mostly saturated to oversaturated in fluids from most parts of the study area (Fig. 3a), and actively deposited in Xolotlan lake.

3.3. Minor and trace elements

The concentrations of 21 minor and trace elements were determined in a sub-set of about 60 samples, and the results are reported in Table 2. On the basis of median values (χ; Table 2), the elements can be divided into 3 groups, i.e., minor elements ($X > 100$ μg/l; B and Sr), trace elements $0{,}1 < X < 100$ μg/l; the majority of the elements and ultra-trace elements ($X < 0.1$ μg/l; Cd and Co).

The wide minimum–maximum range for the majority of the elements (Table 2) is evidence of diverse water/rock interaction regimes and/or multiplicity of source processes. Inspection of Fig. 6, where the mean abundances of trace elements in the different water groups are compared, elicits the following suggestions:

(i) Surface waters (Group 1 and Group 2) are (with a few exceptions) characterized by lower trace element abundances than groundwaters, suggesting that atmospheric deposition is a minor source of trace elements. Otherwise the highest concentrations of Ni (~40 μg/l) and Cu (~10 μg/l), and significant Al concentrations (~70 μg/l) are found in the Xolotlan lake. Sample 22(12) is an exception, its composition appearing to be influenced by the nearby thermal spring of Tipitata, showing anomalous, higher contents of Al, Fe and Zn. Xolotlan lake is a reservoir, where groundwater is an important source. The lake is surrounded by a group of important aquifers which discharge into the lake, and discharge occurs discontinuously via the Tipitapa river. Dissolved salts and possibly metals are contributed by groundwater, and subsequent evaporation increases their concentration (Krasny, 1995). Further increase of TDS and metals is exacerbated by discharge

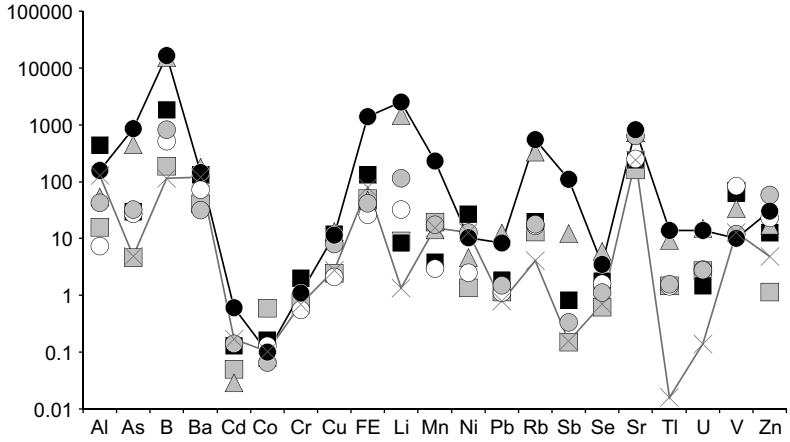

Fig. 6. Trace element mean abundances in the different water groups. Symbols as in Fig. 2.

of sewage from Managua city and residual irrigation water, which contains pesticide and fertilizer residuals. Nickel is found in all soils and is emitted by volcanoes. Nickel can combine with Cl, S and O to form compounds that are soluble in water (see references in Stumm and Morgan, 1996). Although the presence of Ni in Lake Xolotlan might be associated with natural sources, anthropogenic sources are not ruled out; Ni for example is also used in some batteries. Possible sources of Cu are organic and inorganic compounds used in agricultural pesticide sprays. These are used as algaecides, bactericides, fungicides and herbicides.

(ii) The highest concentrations of most trace elements (As, B, Cd, Fe, Li, Mn, Rb, Sb, Tl, U) are found in Cl-rich (Group 6) geothermal waters. This supports the idea of cycling of trace elements in volcanic/hydrothermal processes (e.g., Barnes, 1997), and suggests that volcanic processes may have even more impact on groundwater chemistry than human activities (at least in the study area).

(iii) The trace element concentrations of saline (Group 3) volcanic lakes are close to Group 6 thermal fluids (see As, B, Li, Rb, Tl, U), further supporting the hypothesis that there is a generic link between the two fluid types. The concentrations of the elements Fe, Al, Cd, Mn and Sb are much lower in volcanic lakes than in thermal waters (see Fig. 6 and Table 2), suggesting their removal in the lake's sediments (mostly as Fe and Al oxides and hydroxides) upon cooling of the geothermal waters. This hypothesis is further supported by calculated saturation indices for $Fe(OH)_3$ (amorphous) and Gibbsite (Figs. 3b and c), documenting that most samples are close to saturation with respect to both mineral phases; and it is also in agreement with results of XRD measurements on the lake sediments (Parello, unpublished data), showing that calcite and amorphous phases (likely Fe oxyhydroxides) are ubiquitous. The scavenging of the trace metals Cd, Mn and Sb by surface adsorption on to Fe hydroxides is well documented in the literature (Stumm and Morgan, 1996).

The same information was also provided by factor analysis, which was applied to a subset of 22 selected variables. Four factors, having eigenvalues higher than 1, were extracted and rotated according to the orthogonal Varimax procedure. The loadings of the rotated 4-factor solution are shown in Table 3, along with the variance accounted for by each factor.

Factor analysis attributed 81% of the total variance in the chemistry of groundwaters to 4 factors. Factor 1, which explains 43% of the total variance, clusters T, Na, Cl, Li, B, As, Rb, Sb, Tl Pb and U. Based on the previous discussion (cf. 3.2), the significantly high positive loadings of temperature, Na and Cl on Factor 1 are suggestive of hydrothermal derivation of trace elements clustering into this association of variables, this outcome being supported further by the Cl vs. B and Cl vs. As scatter diagrams (Fig. 7). As such, the two scatter diagrams highlight the considerable impact of volcanic/hydrothermal processes on water chemistry in an active volcanic area; apart from being high in the surface thermal manifestations of geothermal systems (e.g., Group 6 groundwaters), As and B concentrations are above the WHO (WHO, 2001, 1993) recommended limits for drinking water in many surface waters (e.g., Xolotlan lake) and groundwaters. Comparison of Figs. 7a and b

Table 3
Factor analysis for a subset of 22 selected variables, with the variance accounted for by each factor

Factors	1	2	3	4
PH	0.08	0.54	−0.54	−0.19
Na	0.81	0.40	0.35	0.06
Ca	0.01	−0.23	0.84	0.18
Cl	0.84	0.28	0.37	0.09
SO_4	0.16	−0.10	0.67	−0.18
HCO_3	−0.05	0.82	−0.05	0.05
Li	0.97	0.07	0.19	0.04
B	0.81	0.32	0.40	0.12
Al	0.05	0.20	−0.43	0.49
Mn	0.09	−0.03	0.29	0.80
Fe	0.02	0.06	−0.03	0.95
Ni	−0.13	0.60	−0.31	0.10
Cu	0.59	0.59	−0.09	0.37
As	0.95	−0.10	−0.01	−0.08
Rb	0.98	0.04	0.14	−0.02
Sr	0.41	0.13	0.77	0.30
Sb	0.74	−0.30	−0.33	0.01
Ba	0.15	0.53	0.47	0.52
TL	0.97	−0.16	−0.01	0.05
Pb	0.97	0.04	0.08	0.17
U	0.97	0.00	0.19	0.06
T	0.76	−0.41	−0.13	0.07
Expl. var	9.36	2.72	3.28	2.47
Prp. totl	0.43	0.12	0.15	0.11

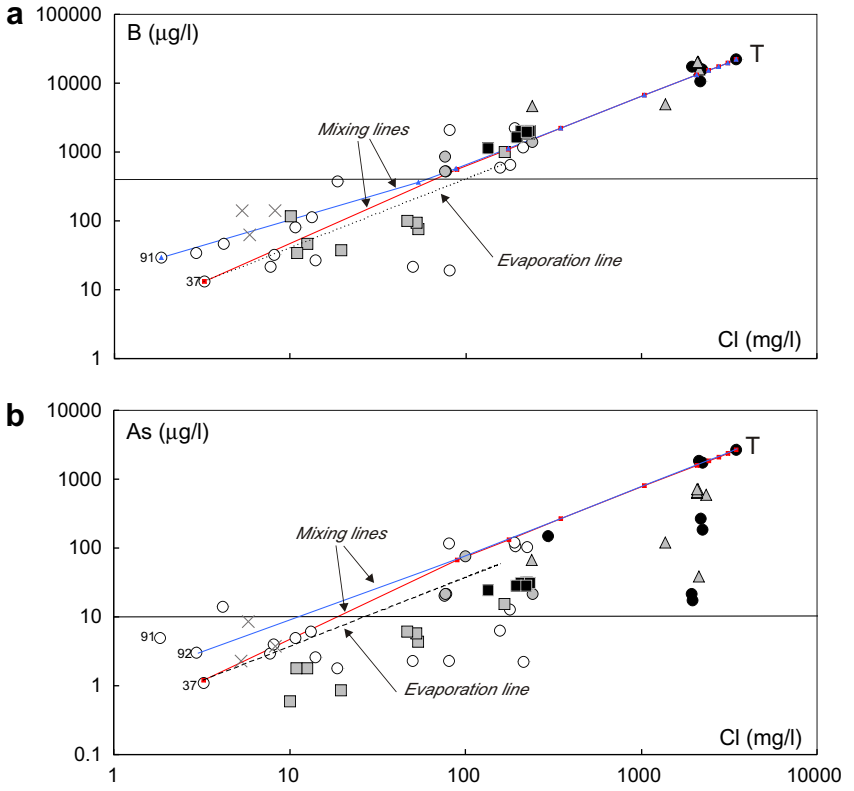

Fig. 7. Scatter diagrams plotting trace elements (B, As) versus Cl concentrations for a sample selection of the different water types. T = thermal end-member. Symbols and mixing lines as in Fig. 2 and Fig. 5a–d.

suggests that – compared with B and Cl–As does not behave conservatively during the mixing and evaporative processes taking place in the hydrological system (i.e. most water samples plot below the mixing and evaporative lines of the model). As most As minerals are unstable at the conditions encountered here (saturation indices being far below 0), adsorption on Fe-oxides is likely to be the main sink for this element.

The association of pH, Na, HCO_3^-, Ni, Cu and Ba is reflected in factor 2, which explains 12% of the total variance. As suggested by the pH vs. HCO_3 and pH vs. Ni scatter diagrams of Fig. 8, this association of variables is difficult to interpret, as at least two processes seem to be involved. In fact, data tend to cluster in Figs. 8a and b on two main compositional trends; trend 1 characterized by negative dependence of HCO_3 and Ni on pH, and trend 2 resulting from the high-HCO_3, high-Ni, high-pH Xolotlan lake waters. While the former simply reflects the increasing groundwater transport of metal cations (e.g., Ni^{2+}) in the acidic conditions typical of gas saturated thermal waters, promoted by increasing amounts of dissolving gaseous CO_2 (which forms HCO_3 by water–rock interaction), the latter seems to require additional C and Ni sources in the Xolotlan lake. Note that these high C contents also lead to the lake being oversaturated with calcite (Fig. 8a). Since Xolotlan lake is the main accumulator of urban and industrial wastewaters from Managua, it is suggested that this waste is the main source of metals (Ni, Cu), whilst decay of its large organic burden might be the source of the high C content.

Factor 3 accounts for 15% of the total variance, and clusters the variables pH, Ca, Ba, Sr and SO_4. It simply reflects the conception of (Group 5) SO_4 thermal waters from the interaction of H_2S-rich hydrothermal steam and meteoric waters (see Figs. 2a and 3c). It should be noted that alkaline-earth elements are typically more abundant than either Na or K in these steam heated groundwaters, as observed in other geothermal regions worldwide (Giggenbach, 1988; Hochstein and Browne, 2000).

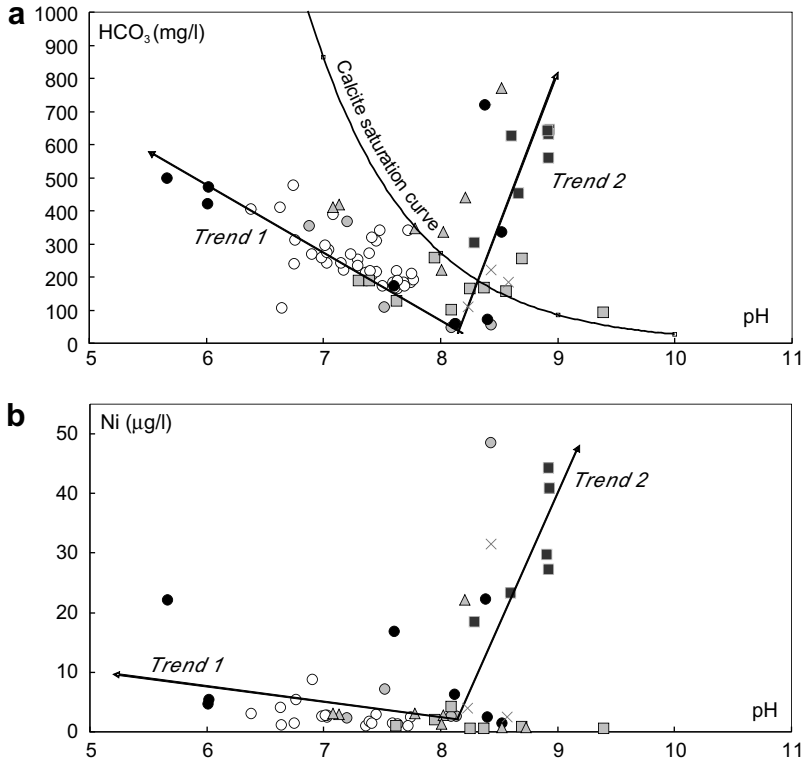

Fig. 8. HCO_3 (a) and Ni (b) versus pH scatter diagrams for a sample selection of the different water types. The arrowed lines describe the main compositional trends. Symbols as in Fig. 2.

Finally, the last factor (11%) is entirely dominated by Fe and Mn; the groundwater transport of the two elements having a similar dependence on redox conditions. Again, the interaction with thermal fluids fosters the development of the most reducing conditions, at which the groundwater release of both Fe and Mn is at its most extensive (Fig. 6).

4. Conclusions

This study provides a preliminary characterization of the geochemical processes governing the chemical maturation of surface waters and groundwaters in the Managua region (Nicaragua), the site of both active volcanism/geothermal activity and relevant pollution. The interpretation of the collected data shows that water chemistry in the Managua area is controlled by a complex interaction between several geochemical processes – namely, evaporation, rock leaching and mixing with saline brines of natural or anthropogenic origin. Evidence is provided that the intense geothermal activity of the region has the most prominent impact on both surface waters (e.g., volcanic lakes) and groundwaters, which develop their intermediate to high salinities and high concentrations of many environmentally-relevant trace elements (As, B, Fe and Mn) as a result of mixing with variable (2–60%) proportions of saline geothermal Na–Cl brines. The interaction with ascending thermal fluids, favoured by the active extensional tectonics of the area also seems to foster leaching of the host rocks and groundwater release of toxic metals (e.g., Ni, Cu). In this context, the significant pollution in the area also contributes to the aquatic cycling of many trace elements, which attain concentrations above the recommended limit (WHO, 1984, 1993) for the elements Ni (~40 µg/l) and Cu (~10 µg/l) in Xolotlan lake. In this case anthropogenic sources play the most important role in water chemistry; metals and other contaminants (i.e. pesticides) have diminished the potential of this lake, that might otherwise have represented a considerable resource for nearby Managua.

References

Aiuppa, A., Bellomo, S., Brusca, L., D'Alessandro, W., Federico, C., 2003a. Natural and anthropogenic factors affecting groundwater quality of an active volcano (Mt. Etna, Italy). Appl. Geochem. 18, 863–882.

Aiuppa, A., D'Alessandro, W., Federico, C., Palumbo, B., Valenza, M., 2003b. The aquatic geochemistry of arsenic in volcanic groundwaters from southern Italy. Appl. Geochem. 18, 1283–1296.

Aydin, A., Nur, A., 1982. Evolution of pull-apart basins and their scale independence. Tectonics 1, 91–105.

Ball, W.P., Nordstrom, D.K., 1991. User's manual for WATEQ4F, with revised thermodynamic database and test cases for calculating speciation of major, trace, and redox elements in natural waters. US Geol. Surv. Open File Rep., 91–183.

Barnes, H.L., 1997. Geochemistry of Hydrothermal Ore Deposits, third ed. Wiley, New York.

Burkart, B., Self, S., 1985. Extension and rotation of crustal blocks in northern Central America and effect on the volcanic arc. Geology 13, 22–26.

Carr, M.J., 1984. Symmetrical and segmented variation of physical and geochemical characteristics of the Central American volcanic front. J. Volc. Geotherm. Res. 20, 231–252.

Carr, M.J., Feigenson, M.D., Patino, L.C., Walker, J.A., 2003. Volcanism and geochemistry in Central America: progress and problems. In: Eiler, J.M. (Eds), Inside the subduction factory, vol. 138. Geophys. Monogr. Ser., pp. 153–174.

Couch, R., Woodcock, S., 1981. Gravity structure of the continental margins of southwestern Mexico and northwestern Guatemala. J. Geophys. Res. 86, 1829–1840. Abstract-INSPEC.

Delmelle, P., 2003. Environmental impacts of tropospheric volcanic gas plumes. In: Oppenheimer, C., Pyle, D.M., Barclay, J. (Eds.), Volcanic degassing, vol. 213. Geological Society, Special Publication, London, pp. 381–399.

DeMets, C., 2001. A new estimate for present-day Cocos–Caribbean Plate motion; implications for slip along the Central American volcanic arc. Geophys. Res. Lett. 28, 4043–4046.

Giggenbach, W.F., 1988. Geothermal solute equilibria. Derivation of Na–K–Mg–Ca geoindicators. Geochim. Cosmochim. Acta 52, 2749–2765.

Hochstein, M.P., Browne, P.R.L., 2000. Surface manifestations of geothermal systems with volcanic heat sources. In: Sugurdsson, H. (Ed.), Encyclopaedia of Volcanoes. Academic Press, pp. 835–855.

Istituto Vulcanologico, A.C., U.R.S.S., 1983. Reporte preliminar del estudio vulcanologico del volcan Momotombo y sus alrededores. Instituto Nicaraguese De Estudios Territoriales, Managua.

Krasny, J., 1995. Hidrogeología de la Zona Pacífica de Nicaragua,nota esplicativa al mapa hidrogeologico a escala 1:250,000, INETER-GTZ.

Martinez, B.W., Noguera, B.E., 1992. Geological framework of earthquake occurrence in Nicaragua, Central America. J. Geol. Soc. 98, 165–176.

McBirney, A.R., Williams, H., 1965. Volcanic history of Nicaragua. Univ. Calif. Publ. Geol. Sci. 55, 1–65.

Parkhurst, D.L., 1995. User's Guide to PHREEQC-a computer program for speciation, reaction-path, advective-transport, and inverse geochemical calculations. US Geol. Surv. Water-Resour. Invest. Rep. pp. 95–4227.

Parkhurst, D.L., Appelo, C.A.J., 1999. User's guide to PHREEQC (Version2) – A computer program for speciation, batch-reaction, one-dimensional transport, and inverse geochemical calculations. US Geol. Surv. Water-Resour. Invest. Rep. pp. 99–4259.

Reyes García, C.J., 1977. Análisis de la calidad del agua subterránea en la zona comprendida entre la laguna de Asososca y lago de Managua. Instituto Nicaragüense de Recursos Naturales y del Ambiente (IRENA), Managua.

Rozanski, K., 1999. Water balance of lake Xolotlan. Assessment of groundwater inflow and outflow rates using isotope data. Final Report, IAEA Technical Co-operation Project NIC/8/010, Vienna, Austria.

Stumm, W., Morgan, J.J., 1996. Aquatic Chemistry, third ed., Chemical Equilibria and Rates in Natural Waters Wiley-Interscience, New York.

van Wyk de Vries, B., 1993. Tectonics and magma evolution of Nicaraguan volcanic systems. Ph.D. thesis, The Open University, Milton Keynes, UK.

Walker, J.A., 1984. Volcanic rocks from the Nejapa and Granada cinder cone alignments. Nicaragua. J. Petrol. 25, 299–342.

Walker, J.A., Carr, M.J., Feigenson, M.D., Kalamarides, R.I., 1990. The petrogenetic significance of high-and low-Ti basalts in Central Nicaragua. J. Petrol. 31, 1141–1164.

Wehrmann, H., 2005. Volatile degassing and plinian eruption dynamics of the mafic Fontana Tephra, Nicaragua. Ph.D. thesis, IFM-GEOMAR, Christian-Albrechts Universität zu Kiel.

WHO, 1984. Guidelines for drinking-water quality, second ed. World Health Organization, Geneva.

WHO, 1993. Guidelines for drinking-water quality, second ed. World Health Organization, Geneva.

WHO, 2001. Arsenic in Drinking Water. Fact Sheet 210. World Health Organization, Geneva.